

AE-406

The Decay of Optically Thick Helium  
Plasmas, Taking into Account Ionizing  
Collisions between Metastable  
Atoms or Molecules

J. Stevefelt

This report is intended for publication in a periodical. References may not be published prior to such publication without the consent of the author.



AKTIEBOLAGET ATOMENERGI

STUDSVIK, NYKÖPING, SWEDEN 1970



THE DECAY OF OPTICALLY THICK HELIUM PLASMAS, TAKING  
INTO ACCOUNT IONIZING COLLISIONS BETWEEN METASTABLE  
ATOMS OR MOLECULES

J. Stevefelt

ABSTRACT

The effective recombination rate of a helium afterglow plasma, which is optically thick towards the resonance lines, is calculated from the coupled rate equations for the number densities of free electrons and of metastable atoms or molecules. The model employed is a neutral plasma, consisting of one kind of ions and one kind of metastables. The ions are lost by electron-ion recombination only, with subsequent formation of metastables, which are then deactivated in collisions with free electrons or with other metastables: in the latter case one electron is regained to the free state. When the rate constants for these various processes are time-independent, it is found that after a certain transition time a transient equilibrium between the number densities of electrons and metastables is attained. In a dense afterglow plasma, where the recombination coefficient may be large, the transient equilibrium density of metastables may become significantly higher than the quasi-equilibrium value obtained by equating the time derivative of the metastable density to zero, and the effective recombination coefficient may be reduced by much more than a factor of two.

LIST OF CONTENTS

	<u>Page</u>
1. Introduction	3
2. Physical model	4
3. Solution of differential equation for the ratio $p$	6
4. The transition time	9
5. The effective recombination coefficient	12
Acknowledgements	13
References	14
Captions of figures	15
Figures	

## 1. INTRODUCTION

A large amount of experimental work on electron-ion recombination in helium discharge plasmas has shown that, under current afterglow conditions, the plasma disintegrates in reasonable agreement with the model of collisional-radiative recombination. This model has been worked out in articles by Bates et al. [1], Bates and Khare [2], Bates et al. [3], and Collins [4].

In the theoretical approach of Bates et al. [1] a rate equation is written for each excited level  $n$  of the neutral atom, describing the rate of increase of the population density  $N_n$  with time. Thus an infinite set of coupled differential equations is obtained, which yields the course of the recombination. Except for extremely dense plasmas, the population densities  $N_n$  ( $n \neq 1$ ) are much smaller than the density  $N$  of free electrons, and so the same is valid for the time derivatives of  $N_n$  and  $N$ . This means that a quasi-equilibrium number density is established almost instantaneously for the excited levels, and the time derivatives  $\dot{N}_n$  ( $n \neq 1$ ) occurring in the set of differential equations can be put equal to zero, which greatly simplifies the solution.

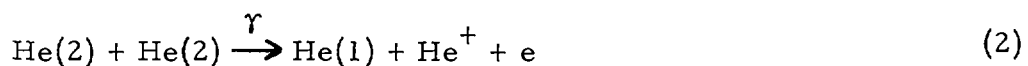
In a later paper by Bates et al. [3] the influence of ionizing collisions between two metastable atoms on the overall recombination rate was taken into account. This calculation was also based on an assumption of quasi-equilibrium number density of metastables, and it was shown that the effective recombination coefficient may then be reduced by at most a factor of two. However, as was pointed out already in the former paper [1], in a plasma which is optically thick to the resonance lines the density of atoms in the quantum level  $n = 2$  may become comparable to the free electron density, and the assumption of quasi-equilibrium metastable density is then no longer justified. This is a common situation in an afterglow plasma, and the

calculation of the metastable density and effective recombination coefficient in such a plasma will be the subject of the present paper.

## 2. PHYSICAL MODEL

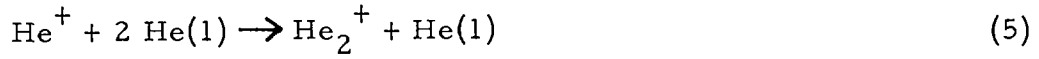
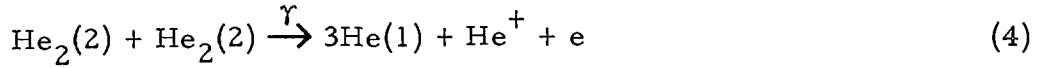
We assume a two-level model of the helium atom or molecule: a ground level with quantum number  $n = 1$ , which for the helium molecule is repulsive, and an excited, metastable level with quantum number  $n = 2$ . In addition, we consider the unbound level  $n = \infty$ . The plasma is neutral, that is, the free electron density is equal to the number density of ions; further, there is just one kind of ions and one kind of metastables (atomic or molecular). The free electrons recombine with the ions in an unspecified way to form a metastable state, and the rate constant for this process is called the recombination coefficient  $\alpha$ . The metastables are deexcited to the ground level in collisions with free electrons with a rate constant  $\beta$ . Finally, two metastables may collide with each other, such that one is deexcited and the other becomes ionized. The rate coefficient for this process is denoted  $\gamma$ . All other processes, such as ambipolar diffusion, are assumed to be negligibly slow. Further, in a first consideration, the three rate constants  $\alpha$ ,  $\beta$ , and  $\gamma$  are assumed to be time-independent.

This simplified model might be applied to several limiting cases. First, when the dominant ion is the atomic  $\text{He}^+$ , the collisional-radiative recombination results in the formation of atomic metastables  $\text{He}(2)$ , which undergo mutual ionizing collisions to again produce atomic ions:



Here, the stabilizing particle  $X$  may be an electron or a neutral

atom. If, on the other hand, only molecular ions  $\text{He}_2^+$  are present in the afterglow, collisional-radiative recombination results in the formation of molecular metastables  $\text{He}_2(2)$ , which, colliding with each other, produce atomic ions, as was demonstrated by Collins and Hurt [5]. If the pressure is high enough, the atomic ions are immediately converted into molecular ions:



Finally, the dominant ion may be  $\text{He}_2^+$ , undergoing dissociative recombination to form atomic metastables  $\text{He}(2)$ :



These metastables may obey the process (2), forming atomic ions, which again, if the pressure is high, are rapidly converted according to (5). In this case we have molecular ions but atomic metastables, and the recombination radiation observed will be atomic line emission.

Denoting the metastable density by  $M$ , the free electron density by  $N$ , and the time derivatives by  $\dot{M}$  and  $\dot{N}$ , this physical model leads to the coupled rate equations

$$\dot{M} = \alpha N^2 - \beta MN - 2\gamma M^2 \quad (7)$$

$$\dot{N} = -\alpha N^2 + \gamma M^2 \quad (8)$$

If  $M$  is substituted against the ratio  $p = M/N$ , the rate equations become

$$\dot{p} = -N[\gamma p^3 + 2\gamma p^2 - (\alpha - \beta)p - \alpha] \quad (9)$$

$$\dot{N} = -N^2(\alpha - \gamma p^2) \quad (10)$$

From eq. (10) it is seen that the effective recombination coefficient is given by the expression

$$\alpha_{\text{eff}} = \alpha - \gamma p^2 \quad (11)$$

### 3. SOLUTION OF DIFFERENTIAL EQUATION FOR THE RATIO $p$

Next we shall determine the time development of the different particle concentrations. It is then simplest to study the ratio  $p$  between the metastable density  $M$  and the free electron density  $N$ . The rate equations (9) and (10) can be combined into one second-order differential equation for the density ratio  $p$ :

$$\ddot{p} = \frac{2\gamma p^2 + 4\gamma p + \beta}{\gamma p^3 + 2\gamma p^2 - (\alpha - \beta)p - \alpha} \dot{p}^2 \quad (12)$$

After one integration, equation (12) yields

$$\dot{p} = C \prod_{i=1}^3 |p - p_i|^{A_i} \quad (13)$$

$p_1$ ,  $p_2$ , and  $p_3$  are the solutions of the equation

$$\gamma p^3 + 2\gamma p^2 - (\alpha - \beta)p - \alpha = 0 \quad (14)$$

and  $A_1$ ,  $A_2$ , and  $A_3$  are determined by the identity

$$\frac{2\gamma p^2 + 4\gamma p + \beta}{\gamma p^3 + 2\gamma p^2 - (\alpha - \beta)p - \alpha} = \frac{A_1}{p - p_1} + \frac{A_2}{p - p_2} + \frac{A_3}{p - p_3} \quad (15)$$

The integration constant  $C$ , appearing in equation (13), is determined by equation (9) together with the initial values  $N_0$  and  $p_0$  at time zero.

It is seen that the values of  $p_i$  and  $A_i$  ( $i = 1, 2, 3$ ) are functions of the two ratios

$$a = \alpha/\gamma, \quad b = \beta/\gamma$$



only. Further, if  $b \leq 1$ , a condition which is always fulfilled according to the data published by Bates et al. [3] and Collins [6], all the zeros  $p_i$  are real: one is positive and two are negative. Equation (9) can be written

$$\dot{p} = -\gamma N(p - p_1)(p - p_2)(p - p_3) \quad (16)$$

where  $p_1$  is the positive solution. The factors  $(p - p_2)$  and  $(p - p_3)$  are then positive, since the density ratio  $p$ , as well as  $\gamma$  and  $N$ , are positive quantities. Hence,

$$\dot{p} > 0 \text{ if } p < p_1, \text{ and } \dot{p} < 0 \text{ if } p > p_1,$$

and during the whole afterglow,  $p$  tends to approach the positive solution  $p_1$ . Computed values of  $p_i$  and  $A_i$  are given in tables 1-3 for different values of  $a$  and  $b$ . The following may be noted:

$$\text{for } a \gg 1, \quad b \leq 1 \quad p_1 \rightarrow \sqrt{a} \quad (17)$$

$$\text{for } a \ll 1, \quad b \lesssim a \quad p_1 \rightarrow \sqrt{a/2} \quad (18)$$

$$\text{for } a \ll 1, \quad b \gg a \quad p_1 \rightarrow a/b = \alpha/\beta \quad (19)$$

$$\text{and, in addition} \quad A_1 \gtrsim 1 \quad (20)$$

$$A_1 + A_2 + A_3 = 2 \quad (21)$$

$$p_1 + p_2 + p_3 = -2 \quad (22)$$

Table 1.  $b = 0$

a	$p_1$	$p_2$	$p_3$	$A_1$	$A_2$	$A_3$
0.0191	0.1	-0.10	- 2.00	1.022	0.973	0.005
0.0733	0.2	-0.18	- 2.02	1.039	0.942	0.018
0.417	0.5	-0.40	- 2.10	1.071	0.830	0.098
1.50	1.0	-0.63	- 2.37	1.091	0.612	0.297
5.33	2.0	-0.85	- 3.15	1.091	0.297	0.612
29.2	5.0	-0.97	- 6.03	1.063	0.066	0.871
109	10.0	-0.99	-11.01	1.039	0.018	0.942

Table 2.  $b = 0.5$

a	$P_1$	$P_2$	$P_3$	$A_1$	$A_2$	$A_3$
0.0645	0.1	-0.37	- 1.73	1.063	1.117	- 0.181
0.157	0.2	-0.45	- 1.75	1.092	1.051	- 0.143
0.583	0.5	-0.62	- 1.88	1.125	0.860	0.015
1.75	1.0	-0.79	- 2.21	1.130	0.558	0.312
5.67	2.0	-0.92	- 3.08	1.112	0.236	0.652
29.6	5.0	-0.98	- 6.02	1.070	0.050	0.881
110	10.0	-1.00	-11.00	1.041	0.014	0.945

Table 3.  $b = 1.0$

a	$P_1$	$P_2$	$P_3$	$A_1$	$A_2$	$A_3$
0.110	0.1	-1.00	- 1.10	1.076	9.091	-8.167
0.240	0.2	-1.00	- 1.20	1.119	4.167	-3.286
0.750	0.5	-1.00	- 1.50	1.167	1.333	-0.500
2.00	1.0	-1.00	- 2.00	1.167	0.500	0.333
6.00	2.0	-1.00	- 3.00	1.133	0.167	0.700
30.0	5.0	-1.00	- 6.00	1.076	0.033	0.891
110	10.0	-1.00	-11.00	1.043	0.009	0.948

When the density ratio  $p$  is closely equal to  $p_1$ , we have what is generally called a "transient equilibrium" between the concentrations of free electrons and metastables. The rate of plasma decay under this condition will be discussed below. First, however, we shall calculate the time of transition from the initial value  $p_0$  to the asymptotic value  $p_1$ . It will be shown that this transition time is much shorter than the characteristic decay time for the electron density.

#### 4. THE TRANSITION TIME

Equation (13) for  $p$  can be solved exactly, provided that the exponents  $A_i$  are integers. One such case is in the limit of large  $a$ , for all values of  $b \leq 1$ , where

$$A_1 = 1, \quad A_2 = 0, \quad A_3 = 1$$

Comparing equations (13) and (16) one finds

$$C = - \frac{\gamma N_o (p_o - p_1)}{|p_o - p_1|^{A_1} (p_o - p_2)^{A_2 - 1} (p_o - p_3)^{A_3 - 1}} \quad (23)$$

where  $N_o$  and  $p_o$  are taken at the time  $t_o$ . Hence,

$$C < 0 \quad \text{if} \quad p_o > p_1$$

$$\text{and } C > 0 \quad \text{if} \quad p_o < p_1$$

For large  $a$ , equation (13) may then be written

$$\dot{p} = - |C| (p - p_1)(p - p_3) \quad (24)$$

with the solution

$$\frac{p - p_1}{p - p_3} = \frac{p_o - p_1}{p_o - p_3} e^{-(t - t_o)/\tau} \quad (25)$$

and where the characteristic time  $\tau$  is

$$\tau = \frac{1}{(p_1 - p_3) |C|} \quad (26)$$

Inserting asymptotic values for  $p_i$ , this expression becomes

$$\tau = \frac{1}{2\gamma N_o (p_o + 1) \sqrt{a}} = \frac{1}{2 \sqrt{\alpha\gamma} (M_o + N_o)} \quad (27)$$

Also when  $a$  and  $b$  are both small, the exponents  $A_i$  are integers:

$$A_1 = 1, \quad A_2 = 1, \quad A_3 = 0$$

The solution for  $p$  is then again given by the expression (25), with  $p_3$  replaced by  $p_2$ , and with

$$\tau = \frac{1}{(p_1 - p_2) |C|} = \frac{1}{\gamma N_0 (p_0 + 2) \sqrt{2} a} = \frac{1}{\sqrt{2} \alpha \gamma (M_0 + 2N_0)} \quad (28)$$

It is seen that the characteristic transition times  $\tau$  for these two considered cases, given by the expressions (27) and (28), respectively, differ by at most a factor  $\sqrt{2}$ : this maximum difference occurs for  $p_0 = 0$ .

In the general case, when  $A_i$  are not integers, it is convenient to define a characteristic transition time for the quasi-exponential approach in time of  $p$  to the asymptotic value  $p_1$ :

$$\tau = - \frac{p - p_1}{\dot{p}} \quad (29)$$

We want to evaluate this transition time for the situation where the density ratio  $p$  is only "slightly" deviating from the "transient equilibrium" value  $p_1$ , which could occur for instance when the rate coefficients  $\alpha$ ,  $\beta$ , and  $\gamma$  vary slowly in time. Inserting the expressions (13) and (23), and approximating  $A_1 = 1$ ,  $p = p_1$ , we obtain

$$\tau = \frac{1}{N_0 \sqrt{\alpha \gamma}} f(a, b, p_0) \quad (30)$$

where the function  $f(a, b, p_0)$  is given by

$$f(a, b, p_0) = \frac{\sqrt{a}}{(p_0 - p_2)^{1-A_2} (p_0 - p_3)^{1-A_3} (p_1 - p_2)^{A_2} (p_1 - p_3)^{A_3}} \quad (31)$$

It is easily verified, by inspection of tables 1-3, that the expressions (30) and (31) develop into the expressions (27) and (28) for the two respective special cases considered above. For fixed values  $a$  and  $b$ ,  $\tau$  has its maximum value for  $p_0 = 0$ : this value then represents an upper bound for the transition time  $\tau$  at those particular values  $a$ ,  $b$ ,  $\gamma$ , and  $N_0$ . The function  $f(a, b, p_0 = 0)$  is shown graphically in Fig. 1: its variation is quite small, and

$$f(a, b, 0) \lesssim 1/2$$

Hence

$$\tau < \frac{1}{2N_0 \sqrt{\alpha r}} \quad (32)$$

From equation (16)  $\tau$  may be expressed in terms of the instantaneous electron density  $N$ , if again  $p$  is nearly equal to  $p_1$ :

$$\tau = \frac{1}{\gamma N (p_1 - p_2)(p_1 - p_3)} \quad (33)$$

Rewriting this expression as

$$\tau = \frac{1}{\gamma N (a + \sqrt{a})} g(a, b) \quad (34)$$

it is found that the function

$$g(a, b) = \frac{a + \sqrt{a}}{(p_1 - p_2)(p_1 - p_3)} \quad (35)$$

is very similar to the function  $f(a, b, p_0 = 0)$ , in particular it varies slowly with  $a$  and  $b$ . Common features of the two functions are

$$f, g \rightarrow 1/2 \quad \text{for } a \rightarrow \infty \quad (36)$$

$$f, g \lesssim 1/2 \quad (37)$$

$$f, g \rightarrow \sqrt{2}/4 \quad \text{for } a \rightarrow 0, b = 0 \quad (38)$$

$$f, g \propto \sqrt{a} \quad \text{for small } a, b = 1 \quad (39)$$

From the upper bound of  $g$  it follows that

$$\tau \leq \frac{1}{2\gamma N(a + \sqrt{a})} = \frac{1}{2N(\alpha + \sqrt{\alpha\gamma})} \quad (40)$$

In a helium afterglow experiment, the reaction rate coefficients  $\alpha$ ,  $\beta$ , and  $\gamma$  cannot be expected to be time-independent constants. However, their time variation is quite slow, and in any case not faster than the variation in electron density, which might be expressed as a characteristic time for quasi-exponential decay (during a short time interval):

$$\tau_N \frac{N_0}{N} - \frac{N}{N_0} = \frac{1}{\alpha_{\text{eff}} N} - \frac{1}{\alpha N} = \frac{1}{\alpha\gamma N}$$

it is seen, by comparison with the expression (40), that

$$\tau \ll \tau_N$$

In general, between five and ten characteristic times for approaching "transient equilibrium" between the densities of metastables and free electrons have elapsed before the electron density has decayed to  $1/e$  of its initial value  $N_0$ . This also means that, even in an afterglow, where the recombination coefficient varies in time, the density ratio  $p$  between metastables and free electrons relaxes to a value close to the transient equilibrium value  $p_1$ , which is a function of the rate coefficients  $\alpha$ ,  $\beta$ , and  $\gamma$  only. The rate of plasma decay under such a transient equilibrium will next be discussed.

## 5. THE EFFECTIVE RECOMBINATION COEFFICIENT

The free electron density decays at a rate given by the equations (8) or (10). Under "transient equilibrium" the positive solution  $p_1$  of equation (14) is to be inserted for the density ratio  $p$  in the expression (10). The resulting effective recombination coefficients  $\alpha_{\text{eff}}$ , as de-

defined by the expression (11), are presented in Fig. 2 as the ratio  $\alpha_{\text{eff}}/\alpha$  versus  $a = \alpha/\gamma$ , and with  $b = \beta/\gamma$  as parameter.

It is especially noted that, for small  $a$ ,  $b \neq 0$ , the ratio  $\alpha_{\text{eff}}/\alpha$  tends to unity, exactly like the result obtained under the quasi-equilibrium approximation for the metastable density: for the expression (19) is valid in both cases. For larger values of the ratio  $a = \alpha/\gamma$ , however, it is easily seen from the rate equation (7) that, since the time derivative  $\dot{M}$  in reality is negative and different from zero, the metastable density  $M$  must be larger than the quasi-equilibrium value obtained from the approximation  $\dot{M} = 0$ . Thus, for large  $a$  the ratio  $\alpha_{\text{eff}}/\alpha$  decreases like  $1/\sqrt{a}$ , while in the quasi-equilibrium approximation it approaches the value  $1/2$ .

Inserting experimental values of  $\beta$  and  $\gamma$  for helium, reported by Bates et al. [3] and Collins [6]:

$$\beta = 6.4 \cdot 10^{-16} \text{ m}^3/\text{sec}, \quad \gamma = 1.85 \cdot 10^{-15} \text{ m}^3/\text{sec}$$

it is seen that the ratio  $\alpha_{\text{eff}}/\alpha$  is reduced to about one half even for recombination coefficients  $\alpha$  as small as  $10^{-15} \text{ m}^3/\text{sec}$ . This implies that ionizing collisions between metastable atoms or molecules are of importance in practically all laboratory helium afterglow plasmas, a fact which must be taken into account in any experimental determination of the recombination coefficient for helium ions, based upon afterglow measurements of the decay of electron density.

#### ACKNOWLEDGEMENTS

The author wishes to thank Dr. K. Nygaard and Dr. S. Palmgren for many stimulating and valuable discussions during the course of this work

REFERENCES

1. BATES, D.R., KINGSTON, A.E. and MC WHIRTER, R.W.P.  
Recombination between electrons and atomic ions. 1 and 2.  
Proc. roy. soc. 267A (1962) p. 297 and 270A (1962) p. 155.
2. BATES, D.R. and KHARE, S. P.  
Recombination of positive ions and electrons in a dense neutral gas.  
Proc. phys. soc. 85 (1965) p. 231.
3. BATES, D.R., BELL, K. L. and KINGSTON A.E.  
Excited atoms in decaying optically thick plasmas.  
Proc. phys. soc. 91 (1967) p. 288.
4. COLLINS, C.B.  
Collisional-radiative recombination of ions and electrons  
in high-pressure plasmas in which the electron temperature  
exceeds the gas temperature.  
Phys. rev. 177 (1969) p. 254.
5. COLLINS, C.B. and HURT, W.B.  
Late-time source of atomic light in the helium afterglow.  
Phys. rev. 177 (1969) p. 257.
6. COLLINS, C.B.  
Chemistry of the low pressure helium afterglow.  
Phenomena in ionized gases. 9th Int. Conf. Bucharest  
Aug. 31 - Sept. 6, 1969, p.51



CAPTIONS OF FIGURES

Fig. 1 A graph of the function  $f(a, b, p_0 = 0)$  versus  $a$  with  $b$  as parameter.

Fig. 2 A graph of the recombination coefficient ratio  $\alpha_{\text{eff}}/\alpha$  versus  $a$  with  $b$  as parameter.



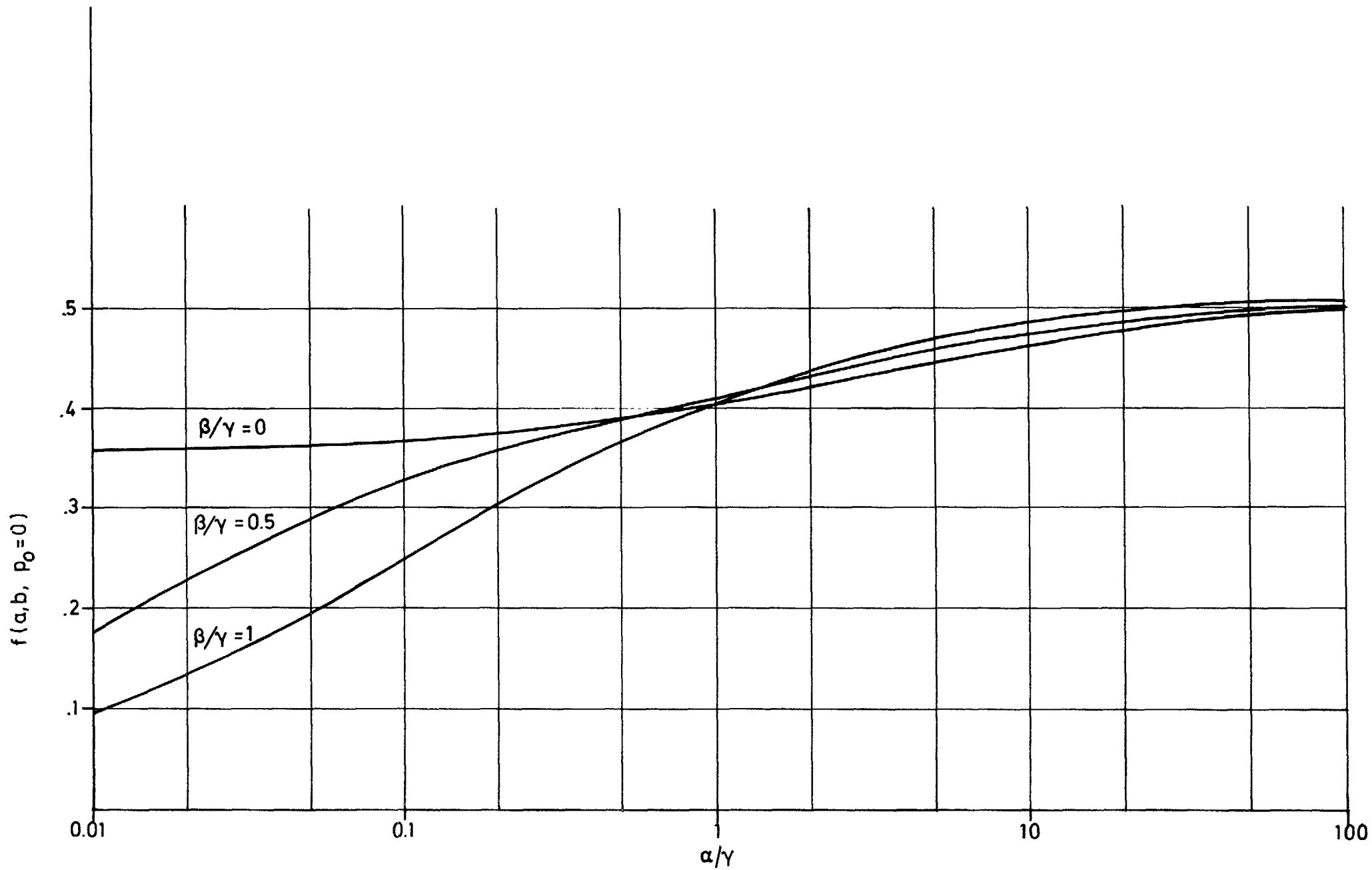


FIGURE 1

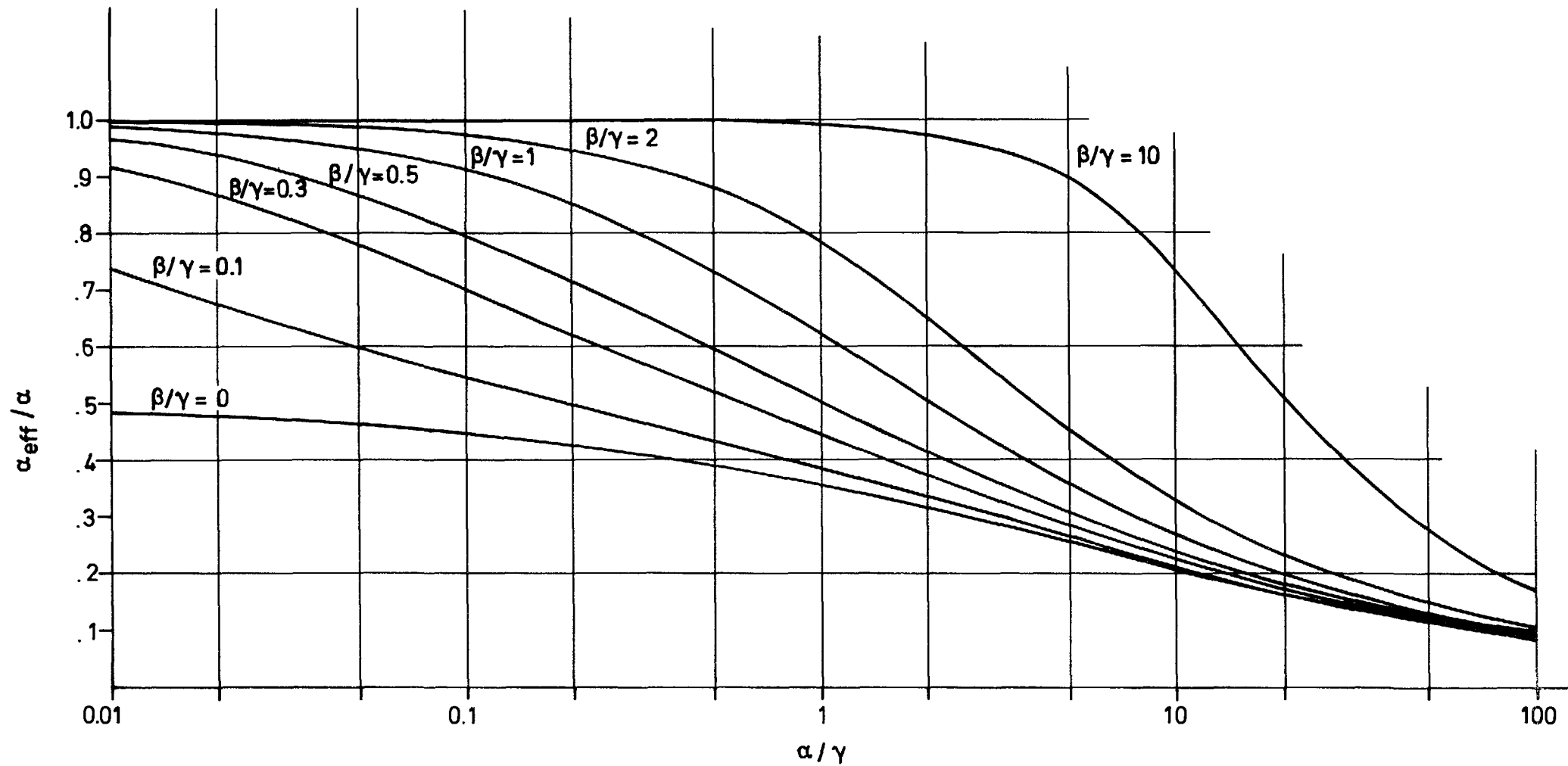


FIGURE 2



LIST OF PUBLISHED AE-REPORTS

1-340 (See back cover earlier reports.)

341. Nonlinear dynamic model of power plants with single-phase coolant reactors. By H. Vollmer. 1968. 26 p. Sw. cr. 10:-.
342. Report on the personnel dosimetry at AB Atomenergi during 1967. By J. Carlsson and T. Wahlberg. 1968. 10 p. Sw. cr. 10:-.
343. Friction factors in rough rod bundles estimated from experiments in partially rough annuli - effects of dissimilarities in the shear stress and turbulence distributions. By B. Kjellström. 1968. 22 p. Sw. cr. 10:-.
344. A study of the resonance interaction effect between  $^{238}\text{U}$  and  $^{239}\text{Pu}$  in the lower energy region. By H. Häggblom. 1968. 48 p. Sw. cr. 10:-.
345. Application of the microwave discharge modification of the Wilzbach technique for the tritium labelling of some organics of biological interest. By T. Gosztonyi. 1968. 12 p. Sw. cr. 10:-.
346. A comparison between effective cross section calculations using the intermediate resonance approximation and more exact methods. By H. Häggblom. 1969. 64 p. Sw. cr. 10:-.
347. A parameter study of large fast reactor nuclear explosion accidents. By J. R. Wiesel. 1969. 34 p. Sw. cr. 10:-.
348. Computer program for inelastic neutron scattering by an anharmonic crystal. By L. Bohlin, I. Ebbsjö and T. Höglberg. 1969. 52 p. Sw. cr. 10:-.
349. On low energy levels in  $^{185}\text{W}$ . By S. G. Malmkog, M. Höjeberg and V. Berg. 1969. 18 p. Sw. cr. 10:-.
350. Formation of negative metal ions in a field-free plasma. By E. Larsson. 1969. 32 p. Sw. cr. 10:-.
351. A determination of the 2 200 m/s absorption cross section and resonance integral of arsenic by pile oscillator technique. By E. K. Sokolowski and R. Bladh. 1969. 14 p. Sw. cr. 10:-.
352. The decay of  $^{190}\text{Os}$ . By S. G. Malmkog and A. Bäcklin. 1969. 24 p. Sw. cr. 10:-.
353. Diffusion from a ground level point source experiment with thermoluminescence dosimeters and Kr 85 as tracer substance. By Ch. Gyllander, S. Hoffman and U. Widemo. 1969. 23 p. Sw. cr. 10:-.
354. Progress report, FFN, October 1, - September 30, 1968. By T. Wiedling. 1969. 35 p. Sw. cr. 10:-.
355. Thermodynamic analysis of a supercritical mercury power cycle. By A. S. Roberts, Jr. 1969. 25 p. Sw. cr. 10:-.
356. On the theory of compensation in lithium drifted semiconductor detectors. By A. Lauber. 1969. 45 p. Sw. cr. 10:-.
357. Half-life measurements of levels in  $^{215}\text{As}$ . By M. Höjeberg and S. G. Malmkog. 1969. 14 p. Sw. cr. 10:-.
358. A non-linear digital computer model requiring short computation time for studies concerning the hydrodynamics of the BWR. By F. Reisch and G. Vayssier. 1969. 38 p. Sw. cr. 10:-.
359. Vanadium beta emission detectors for reactor in-core neutron monitoring. By I. O. Andersson and B. Söderlund. 1969. 26 p. Sw. cr. 10:-.
360. Progress report 1968. Nuclear chemistry. 1969. 38 p. Sw. cr. 10:-.
361. A half-life measurement of the 343.4 keV level in  $^{175}\text{Lu}$ . By M. Höjeberg and S. G. Malmkog. 1969. 10 p. Sw. cr. 10:-.
362. The application of thermoluminescence dosimeters to studies of released activity distributions. By B.-I. Rudén. 1969. 36 p. Sw. cr. 10:-.
363. Transition rates in  $^{141}\text{Dy}$ . By V. Berg and S. G. Malmkog. 1969. 32 p. Sw. cr. 10:-.
364. Control rod reactivity measurements in the Ägesta reactor with the pulsed neutron method. By K. Björus. 1969. 44 p. Sw. cr. 10:-.
365. On phonons in simple metals II. Calculated dispersion curves in aluminium. By R. Johnson and A. Westin. 1969. 124 p. Sw. cr. 10:-.
366. Neutron elastic scattering cross sections. Experimental data and optical model cross section calculations. A compilation of neutron data from the Studsvik neutron physics laboratory. By B. Holmqvist and T. Wiedling. 1969. 212 p. Sw. cr. 10:-.
367. Gamma radiation from fission fragments. Experimental apparatus - mass spectrum resolution. By J. Higbie. 1969. 50 p. Sw. cr. 10:-.
368. Scandinavian radiation chemistry meeting, Studsvik and Stockholm, September 17-19, 1969. By H. Christensen. 1969. 34 p. Sw. cr. 10:-.
369. Report on the personnel dosimetry at AB Atomenergi during 1968. By J. Carlsson and T. Wahlberg. 1969. 10 p. Sw. cr. 10:-.
370. Absolute transition rates in  $^{192}\text{Ir}$ . By S. G. Malmkog and V. Berg. 1969. 16 p. Sw. cr. 10:-.
371. Transition probabilities in the  $1/2^+(631)$  Band in  $^{235}\text{U}$ . By M. Höjeberg and S. G. Malmkog. 1969. 18 p. Sw. cr. 10:-.
372. E2 and M1 transition probabilities in odd mass Hg nuclei. By V. Berg, A. Bäcklin, B. Fogelberg and S. G. Malmkog. 1969. 19 p. Sw. cr. 10:-.
373. An experimental study of the accuracy of compensation in lithium drifted germanium detectors. By A. Lauber and B. Malmsten. 1969. 25 p. Sw. cr. 10:-.
374. Gamma radiation from fission fragments. By J. Higbie. 1969. 22 p. Sw. cr. 10:-.
375. Fast neutron elastic and inelastic scattering of vanadium. By B. Holmqvist, S. G. Johansson, G. Lodin and T. Wiedling. 1969. 48 p. Sw. cr. 10:-.
376. Experimental and theoretical dynamic study of the Ägesta nuclear power station. By P. Å. Bliselius, H. Vollmer and F. Åkerhielm. 1969. 39 p. Sw. cr. 10:-.
377. Studies of Redox equilibria at elevated temperatures 1. The estimation of equilibrium constants and standard potentials for aqueous systems up to 374°C. By D. Lewis. 1969. 47 p. Sw. cr. 10:-.
378. The whole body monitor HUGO II at Studsvik. Design and operation. By L. Devell, I. Nilsson and L. Venner. 1970. 26 p. Sw. cr. 10:-.
279. ATOSPHERIC DIFFUSION. Investigations at Studsvik and Ägesta 1960-1963. By L.-E. Häggblom, Ch. Gyllander and U. Widemo. 1969. 91 p. Sw. cr. 10:-.

380. An expansion method to unfold proton recoil spectra. By J. Kockum. 1970. 20 p. Sw. cr. 10:-.
381. The 93.54 keV level  $^{84}\text{Sr}$ , and evidence for 3-neutron states above  $N=50$ . By S. G. Malmkog and J. McDonald. 1970. 24 p. Sw. cr. 10:-.
382. The low energy level structure of  $^{211}\text{Fr}$ . By S. G. Malmkog, V. Berg, A. Bäcklin and G. Hedin. 1970. 24 p. Sw. cr. 10:-.
383. The drinking rate of fish in the Skagerack and the Baltic. By J. E. Larsson. 1970. 16 p. Sw. cr. 10:-.
384. Lattice dynamics of NaCl, KCl, RbCl and RbF. By G. Raunio and S. Rolandson. 1970. 26 p. Sw. cr. 10:-.
385. A neutron elastic scattering study of chromium, iron and nickel in the energy region 1.77 to 2.76 MeV. By B. Holmqvist, S. G. Johansson, G. Lodin, M. Salama and T. Wiedling. 1970. 26 p. Sw. cr. 10:-.
386. The decay of bound isobaric analogue states in  $^{27}\text{Si}$  and  $^{27}\text{Si}$  using (d, n) reactions. By L. Nilsson, A. Nilsson and I. Bergqvist. 1970. 34 p. Sw. cr. 10:-.
387. Transition probabilities in  $^{187}\text{Os}$ . By S. G. Malmkog, V. Berg and A. Bäcklin. 1970. 40 p. Sw. cr. 10:-.
388. Cross sections for high-energy gamma transition from MeV neutron capture in  $^{208}\text{Pb}$ . By I. Bergqvist, B. Lundberg and L. Nilsson. 1970. 16 p. Sw. cr. 10:-.
389. High-speed, automatic radiochemical separations for activation analysis in the biological and medical research laboratory. By K. Samsahl. 1970. 18 p. Sw. cr. 10:-.
390. Use of fission product Ru-106 gamma activity as a method for estimating the relative number of fission events in U-235 and Pu-239 in low-enriched fuel elements. By R. S. Forsyth and W. H. Blackadder. 1970. 26 p. Sw. cr. 10:-.
391. Half-life measurements in  $^{131}\text{I}$ . By V. Berg and A. Höglund. 1970. 16 p. Sw. cr. 10:-.
392. Measurement of the neutron spectra in FRO cores 5, 9 and PuB-5 using resonance sandwich detectors. By T. L. Andersson and M. N. Qazi. 1970. 30 p. Sw. cr. 10:-.
393. A gamma scanner using a Ge(Li) semi-conductor detector with the possibility of operation in anti-coincidence mode. By R. S. Forsyth and W. H. Blackadder. 1970. 22 p. Sw. cr. 10:-.
394. A study of the 190 keV transition in  $^{141}\text{La}$ . By B. Berg, Å. Höglund and B. Fogelberg. 1970. 22 p. Sw. cr. 10:-.
395. Magnetoacoustic waves and instabilities in a Hall-effect-dominated plasma. By S. Palmgren. 1970. 20 p. Sw. cr. 10:-.
396. A new boron analysis method. By J. Weitman, N. Däverhög and S. Farvolden. 1970. 26 p. Sw. cr. 10:-.
397. Progress report 1969. Nuclear chemistry. 1970. 39 p. Sw. cr. 10:-.
398. Prompt gamma radiation from fragments in the thermal fission of  $^{235}\text{U}$ . By H. Albinsson and L. Lindow. 1970. 48 p. Sw. cr. 10:-.
399. Analysis of pulsed source experiments performed in copper-reflected fast assemblies. By J. Kockum. 1970. 32 p. Sw. cr. 10:-.
400. Table of half-lives for excited nuclear levels. By S. G. Malmkog. 1970. 33 p. Sw. cr. 10:-.
401. Needle type solid state detectors for in vivo measurement of tracer activity. By A. Lauber, M. Wolgast. 1970. 43 p. Sw. cr. 10:-.
402. Application of pseudo-random signals to the Ägesta nuclear power station. By P.-Å. Bliselius. 1970. 30 p. Sw. cr. 10:-.
403. Studies of redox equilibria at elevated temperatures 2. An automatic divided-function autoclave and cell with flowing liquid junction for electrochemical measurements on aqueous systems. By K. Johansson, D. Lewis and M. de Pourbaix. 1970. 38 p. Sw. cr. 10:-.
404. Reduction of noise in closed loop servo systems. By K. Nygaard. 1970. 23 p. Sw. cr. 10:-.
405. Spectral parameters in water-moderated lattices. A survey of experimental data with the aid of two-group formulae. By E. K. Sokolowski. 1970. 22 p. Sw. cr. 10:-.
406. The decay of optically thick helium plasmas, taking into account ionizing collisions between metastable atoms or molecules. By J. Stevfelt. 1970. 18 p. Sw. cr. 10:-.

List of published AES-reports (In Swedish)

1. Analysis by means of gamma spectrometry. By D. Brune. 1961. 10 p. Sw. cr. 6:-.
  2. Irradiation changes and neutron atmosphere in reactor pressure vessels - some points of view. By M. Grounes. 1962. 33 p. Sw. cr. 6:-.
  3. Study of the elongation limit in mild steel. By G. Östberg and R. Attermo. 1963. 17 p. Sw. cr. 6:-.
  4. Technical purchasing in the reactor field. By Erik Jonson. 1963. 64 p. Sw. cr. 8:-.
  5. Ägesta nuclear power station. Summary of technical data, descriptions, etc. for the reactor. By B. Lilliehöök. 1964. 336 p. Sw. cr. 15:-.
  6. Atom Day 1965. Summary of lectures and discussions. By S. Sandström. 1966. 321 p. Sw. cr. 15:-.
  7. Building materials containing radium considered from the radiation protection point of view. By Stig O. W. Bergström and Tor Wahlberg. 1967. 26 p. Sw. cr. 10:-.
- Additional copies available from the Library of AB Atomenergi, Façk, S-611 01 Nyköping 1, Sweden.